

# Development and Assembly of a Flow Cell for Single-Pass Continuous Electroorganic Synthesis Using Laser-Cut Components

Wolfgang Jud,<sup>[a, b]</sup> C. Oliver Kappe,<sup>[a, b]</sup> and David Cantillo\*<sup>[a, b]</sup>

Flow electrolysis cells are essential for the scale up of synthetic organic electrochemistry. We have developed a simple and inexpensive parallel plate flow cell that can be easily assembled using a stack of laser-cut Mylar foils, which act as gaskets, insulating material, interelectrode gap and flow channel. The ease with which the laser-cutting pattern can be customized has enabled the development of interelectrode separators with

mixing geometries, which improve the mass transfer and thus the current efficiency. The performance of the flow electrolysis cell has been evaluated using the anodic decarboxylative methoxylation of diphenylacetic acid as model transformation. Very high conversions and selectivities have been achieved with single-pass processing, with nearly quantitative current efficiency in some cases.

## 1. Introduction

Over the past few years, synthetic organic electrochemistry has been growing in popularity as a green method to perform redox transformations.<sup>[1,2]</sup> In addition to the innate greenness of this methodology, electrochemical reactions are typically safer and less expensive compared to those using conventional oxidizing or reducing agents.<sup>[3]</sup> Thus, the need of sustainable procedures for the preparation of organic molecules has recently boosted a resurgence in this field.<sup>[4]</sup> Yet, organic electrochemistry has still not become a routine laboratory technique. This has been partly due to the previous lack of dedicated laboratory equipment, and the difficulties often encountered to reproduce results from poorly described homemade electrochemical cells reported in the literature.<sup>[5]</sup> In this context, the standardization of organic electrosynthesis equipment has been recently recognized as essential for the development of this field.<sup>[6]</sup> A second issue of conventional batch electrochemical cells (beaker or H-cells) is connected to limitations regarding scalability. Although a certain scale up in batch is possible, reaction volumes of more than a few liters

become problematic.<sup>[7]</sup> Large vessels lack the necessary heat and mass transfer required for an electrochemical reaction to proceed efficiently. Moreover, the electrode area-to-reaction volume ratio, an important parameter that influences the reaction performance, significantly decreases with the increase of scale in batch.<sup>[8]</sup>

Continuous flow electrolysis cells have been shown as essential tools to overcome the issues associated with the scale up of electrochemical synthesis.<sup>[8,9]</sup> In fact, flow cells have been utilized for many years for very large scale electrochemical reactions.<sup>[7]</sup> In a flow electrolysis cell, the electrodes are placed very close to each other, with a distance typically less than 1 mm. The reaction mixture is then flown through the narrow interelectrode gap using a suitable pumping system. This strategy provides a very large electrode surface area to reaction volume ratio. The small interelectrode distance reduces the ohmic drop within the cell, which results in improved energy transfer and higher conductivity. This ultimately leads to higher current efficiencies and lower concentrations of supporting electrolyte required. Flow cells can be operated from a reservoir with electrolyte recirculation or in single-pass mode.<sup>[8,9]</sup> Although electrolyte recirculation is commonly used in industry, single-pass processing enables truly continuous transformations and integration of the electrochemical step with other reactions or work-up procedures in a single stream.<sup>[10]</sup>

Many types of flow cells for organic electrochemistry have been described in the literature.<sup>[8]</sup> The most commonly used is by far the parallel plate arrangement. In this type of setup, as its name suggests, two flat electrodes are placed facing each other with a narrow gap separating them. Turbulence promoters are often introduced in the interelectrode gap to improve the mass transfer of the system.<sup>[7–9]</sup> This is particularly beneficial when low flow rates are applied to the cell. Notably, there is a very limited number of commercially available cells, especially for laboratory scale organic electrosynthesis. Most flow cells utilized in the literature are “in house” constructions. A very commonly used and practical design incorporates an interelectrode

[a] W. Jud, Prof. C. O. Kappe, Dr. D. Cantillo  
Institute of Chemistry  
University of Graz, NAWI Graz  
Heinrichstrasse 28  
8010 Graz (Austria)  
E-mail: david.cantillo@uni-graz.at

[b] W. Jud, Prof. C. O. Kappe, Dr. D. Cantillo  
Center for Continuous Flow Synthesis and Processing (CCFLOW)  
Research Center Pharmaceutical Engineering GmbH (RCPE)  
Inffeldgasse 13  
8010 Graz (Austria)

 Supporting information for this article is available on the WWW under <https://doi.org/10.1002/cmtd.202000042>

 © 2020 The Authors. Published by Wiley-VCH GmbH. This is an open access article under the terms of the Creative Commons Attribution Non-Commercial NoDerivs License, which permits use and distribution in any medium, provided the original work is properly cited, the use is non-commercial and no modifications or adaptations are made.

separator made of a plastic foil, which features a channel to allow the flow of the reaction mixture.<sup>[11]</sup> This type of setup with an “extended channel” is particularly suited for achieving high conversions of materials in a single pass.<sup>[8]</sup>

The construction of many flow electrolysis cells require CNC machining and similar techniques for the construction of the components. In general, they are still considered rather expensive and complex to fabricate. Herein we present a flow electrolysis cell that can be easily assembled without the need of machined parts. The cell consists of two plate electrodes separated by a plastic foil (Mylar) which incorporates a flow channel. The assembly is constructed with further Mylar films, which act as electrode alignment frames, gasketing material to avoid electrolyte leakage, and insulating material. Notably, all the internal Mylar parts of the cell can be easily laser-cut or acquired from inexpensive laser cutting service providers. The end-plates, made of aluminum, can be constructed with a drill and threading taps, again without the need of CNC machining. The performance of the flow electrolysis cell has been demonstrated using the decarboxylative methoxylation of diphenylacetic acid as model.

## 2. Results and Discussion

### 2.1. Flow Electrolysis Cell Assembly

The electrolysis cell followed a typical parallel plate arrangement.<sup>[12]</sup> The setup is relatively simple and can be easily assembled by overlapping a series of polymer foils and the two electrode plates (Figure 1) (detailed instructions are provided in the Supporting Information). All layers, except for the end plates, were made of Mylar foil. Mylar is a polyester plastic manufactured by Dupont with a very good chemical and solvent resistance. Its shape can be readily customized using inexpensive laser-cutting techniques. Mylar is also an excellent insulating and gasket material often used for the construction

of fuel cells.<sup>[13]</sup> Thus, this material choice ensured that the cell is leak-proof and additional gaskets are not required. At the center of the cell a Mylar foil featuring the reaction channel was placed. In the example presented herein a foil with a 0.3 mm thickness was utilized. A wide range of foil thicknesses is commercially available. Thus, the interelectrode distance can be easily tuned. This film acts as the interelectrode separator and, importantly, as flow channel. The shape of the channel could be tuned to optimize the mixing of the reaction mixture, thus acting as a customizable turbulence promoter (*vide infra*). The two electrodes consisted of 5 × 5 cm plates. This is a standard electrode size. Many electrode materials with these dimensions can be purchased from standard commercial vendors. One of the electrodes featured two orifices for the input and the output of the reaction stream (in case of a divided cell setup, holes are drilled into both electrodes). The two electrodes are centered by alignment gaskets, also made of 0.3 mm thick laser-cut Mylar films. Importantly, this cell design is highly flexible toward the electrode thickness. Electrode thicknesses ranging from 0.1 to 6 mm have been successfully implemented. Thicker plates can also be accommodated. For thick electrodes, several alignment gaskets can be stacked (see graphical assembly instructions in the Supporting Information). For the model reaction described below, for example, 10 gaskets (0.3 mm thickness) were used to hold a 3 mm graphite electrode.

The electrical connections to the electrodes were established via current collectors consisting of 2.6 mm diameter pogo-pins. The pogo pins were inserted in a 2.5 mm i.d., 10 mm o.d. tube and fitted to the end-plates, which were made of 10 mm thick aluminum plate. An additional layer of Mylar foil was placed between the electrodes and the end plates (“isolation layer”, Figure 1), to avoid that current can pass through the end plates. Both end plates contained fluidic fittings (1/4-28 UNF) to enable utilization of the setup both as an undivided and a divided cell (see Figure S1). One of the end plates contained M6 threads for the cell assembly with M6

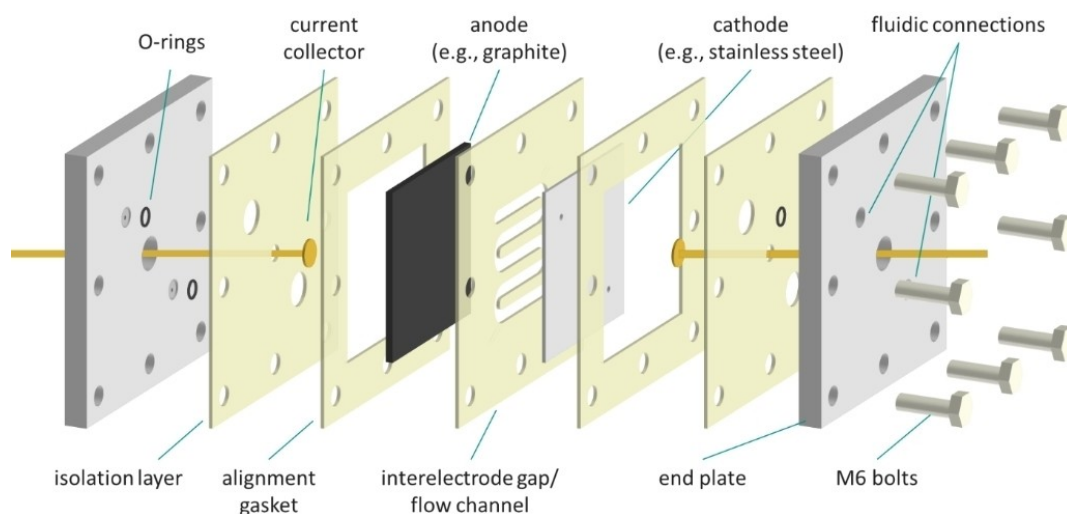


**Figure 1.** Exploded view of the flow electrolysis cell, based on a parallel plate arrangement and consisting of a stack of insulating, chemically resistant Mylar foils (details on all parts dimensions, including SVG files for laser cutting are included in the Supporting Information).

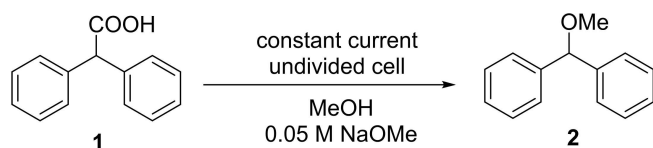
bolts. Alternatively, the two end plates can be built identically with simple 6 mm holes and assembled with bolts and nuts. As mentioned above, the end plates can be constructed using drill and threading taps, without the need of CNC machining.

This setup provides a very high flexibility and modularity to the flow cell. Electrodes of essentially any thickness can be utilized by simply adapting the number of Mylar foils stacked. Both divided and undivided cells can be easily set (Figure S1). If a divided cell is required, two interelectrode gap foils separated by an ion exchange membrane can be implemented (the cell is designed to enable operation in divided and undivided mode; an example of a chemical reaction in undivided mode is shown below). Moreover, the flexibility provided by the laser-cutting of all internal parts enables the tuning of the mixing characteristics of the flow channel. The interelectrode distance can also be easily modified by using a foil with a different thickness. For the model reaction an interelectrode distance of 0.3 mm was utilized.

All internal components of the cell (e.g., Mylar films) were acquired from a standard laser cutting service provider. Details on the dimensions of the cell components are provided in the Supporting Information. Scalable vector graphics (SVG) for the Mylar foils and CAD files for the end plates are also available as Supporting Information to enable reproducing this flow electrolysis cell.

## 2.2. Flow Electrolysis Cell Performance. Decarboxylative Methoxylation of Diphenylacetic Acid

The decarboxylative methoxylation of diphenylacetic acid (**1**) (Scheme 1)<sup>[14]</sup> via a Hofer-Moest reaction<sup>[15]</sup> was selected as model to evaluate the performance of the electrochemical cell. This is a 2-electron oxidation process closely related to the Kolbe electrolysis.<sup>[16]</sup> Initial oxidation of the carboxylate generates an acyloxy radical, which rapidly decomposes releasing CO<sub>2</sub> and an alkyl radical intermediate. A second oxidation step generates the carbocation from the radical, which is then trapped by a nucleophile (methanol in this case). As the first step of the electrochemical reaction leading to the radical intermediate is shared with the Kolbe electrolysis, the typical Kolbe dimers are the main side-products in this transformation.<sup>[15]</sup> Pt anodes combined with salts such as perchlorates or sulfates are well suited for this transformation.<sup>[16]</sup> Carbon anodes also perform well. Indeed, porous carbon materials (e.g. graphite) have been shown to provide good selectivity without the need of the salts mentioned above.<sup>[16]</sup> These types of electrode materials (Pt and C) have also been



**Scheme 1.** Anodic decarboxylative methoxylation of diphenylacetic acid (**1**) used as model reaction.

previously utilized for Hofer-Moest reactions in continuous flow mode.<sup>[17]</sup> In our investigation, graphite was selected as the anode material and stainless steel as the cathode. Preliminary batch experiments showed that these materials perform well in the presence of a catalytic amount of NaOMe as the base for the electrolysis of **1**. Thus, all reactions were carried out using a stock solution of the starting material **1** in MeOH (0.1 M), which contained 0.05 M of NaOMe. In this solution, compound **1** is partially present as its sodium salt, which acts as the actual electroactive species and also provides sufficient conductivity to the solution for the electrochemical reaction to proceed without the need of an additional supporting electrolyte. The cell was operated under constant current in all cases. Constant current electrolysis is the method of choice for electroorganic synthesis on scale in most cases.<sup>[7]</sup> This mode of operation significantly simplifies the technical requirements of the setup, as a three-electrode electrochemical cell or a potentiostat are not required (an inexpensive adjustable power supply can be employed instead).<sup>[17]</sup> Moreover, the reaction selectivity can still be optimized by tuning the current density at the electrodes.

First, the effect of the incorporation of mixing geometries to the flow channel was evaluated. It was expected that mixing geometries would improve the mass-transfer in the reaction solution, potentially increasing the current efficiency. This is typically achieved with the implementation of turbulence promoters in flow electrolysis cells.<sup>[7-9]</sup> Using custom laser-cut interelectrode separators, turbulence can be directly created with the gasketing membrane if the flow channel features passive mixing geometries.<sup>[18]</sup> Thus, three different designs were tested (Figure 2). The first interelectrode separator channel contained a rather simple geometry. Two additional channels with well-known mixing geometries in microreactor technology were applied. In particular, a meandering channel<sup>[19]</sup> and a tangential mixer<sup>[20]</sup> were tested. For this study, the reaction mixture was processed with recirculation of the electrolyte. A reservoir containing 40 mL of the starting solution was prepared, and the mixture pumped through the flow cell with a flow rate of 2.5 mL/min using a peristaltic pump. This rather low flow rate was selected because high flow velocities could result in a turbulent flow, and possibly the effect of the channel geometry could not be appreciated. The output of the cell was connected to the reaction mixture reservoir for recirculation mode. A current of 256 mA (40 mA/cm<sup>2</sup>) was applied. The reaction progress was monitored by HPLC (see Experimental Section for details). Notably, a very high current efficiency was observed in all cases. The channel without mixing geometry showed a current efficiency of 80–90% during the initial 1.6 F/mol, before suffering the expected drop in efficiency at a later stage of the reaction, when the concentration of **1** is low (the reaction requires a theoretical amount of charge of 2 F/mol). The two flow channels incorporating mixing geometries achieved impressive quantitative current efficiencies during the initial 1.6 F/mol (Figure 2). The improvement with respect to the flow channel without mixing geometry is significant, particularly taking into account that the electrode contact surface areas with the mixing geometry are smaller (volumes and contact surface areas for each channel are included in technical

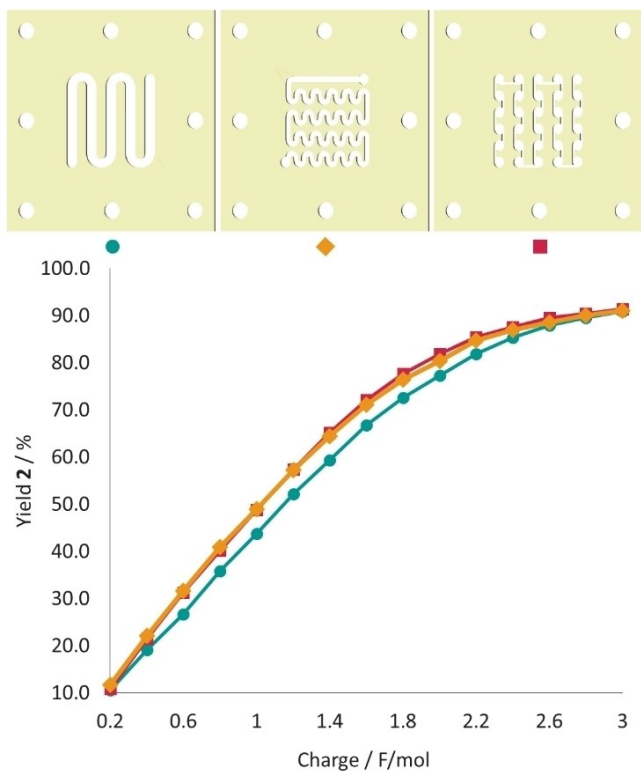


**Figure 2.** Comparison of the performance of interelectrode separator channels with and without mixing structure. HPLC yield of **2** using the flow electrolysis cell in recirculation mode for three designs is shown.

drawings in the Supporting Information). Notably, the flow channels with mixing geometry performed nearly identically. At a later stage of the reaction, the current efficiency was similar for the three channels. A maximum of 90% yield (with 97% conversion of the starting material) was achieved with 3 F/mol, which corresponds to an excess of charge of 50%.

Next, the performance of the flow electrolysis cell was evaluated for single-pass processing of the reaction mixture (Figure 3). A fresh stock solution of **1** was pumped through the flow cell and the solution from the reactor output was collected in a separate vessel. For these experiments, the interelectrode flow channel without mixing geometry was selected. Flow electrolysis cells typically exhibit relatively short residence times (<1 min). This is possible due to the large electrode surface area to volume ratio of the cell (i.e., at any given time only a small volume of the reaction mixture is present in the cell). The short residence time of the reaction in flow enable rapid optimization of the reaction conditions. Thus, a screen of flow rates and amount of charge (Figure 3) was thoroughly performed by gradually tuning the pump flow rate setting and the output current of the power supply. The outcome of the reaction was monitored by collecting aliquots from the reactor output and analyzing it by HPLC (see Experimental Section for details). The reaction performed slightly better at low flow rates, most probably due to the lower current density needed to achieve a given charge within the residence time. Gratifyingly, very high current efficiency and yield of product **2** was obtained

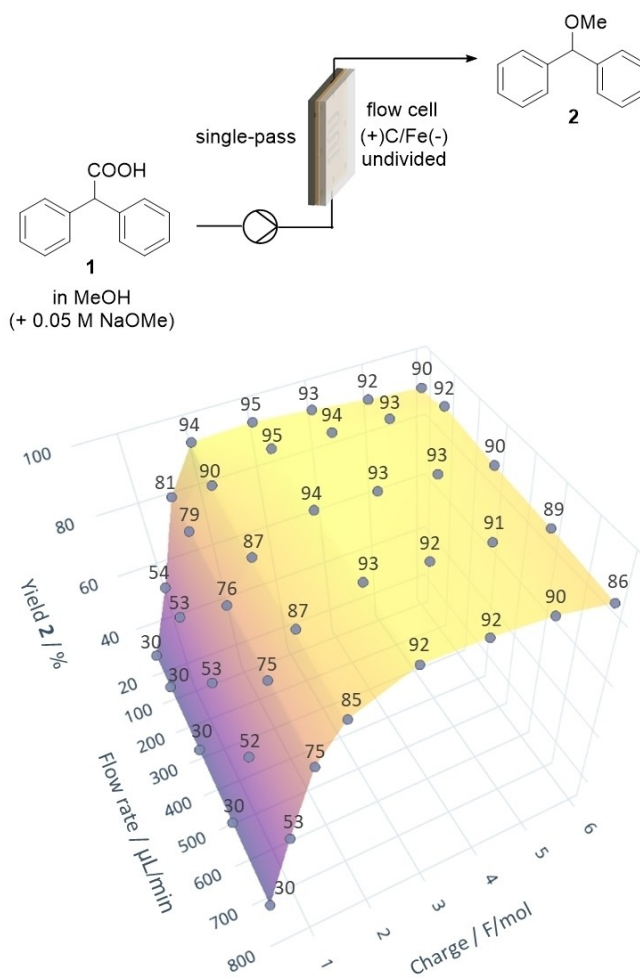


**Figure 3.** Schematic view of the setup utilized for the single-pass continuous flow electrochemical reactions (top) and screen of flow rates and charges evaluated for the model anodic decarboxylative methoxylation of **1**. HPLC yields (215 nm) of **2** are shown.

in all cases. Very good yields (93%–95%) with nearly full conversion of the starting material was achieved with an amount of charge of 2–3 F/mol at flow rates up to 600  $\mu\text{L}/\text{min}$  (<20 s residence time for the 190  $\mu\text{L}$  reactor). Higher amounts of charge (4–6 F/mol) resulted in a moderate decrease in the reaction yield, due to the formation of undesired side-products (most likely degradation of the product due to overoxidation). At the lowest flow rate tested (100  $\mu\text{L}/\text{min}$ ) essentially quantitative current efficiency was achieved (98% conversion with 2 F/mol of charge). This high performance is particularly remarkable for a reaction that produces large amounts of gases ( $\text{CO}_2$  and  $\text{H}_2$  are produced as byproducts). The formation of gases in a flow cell is considered problematic for single pass processing. This issue can be overcome by e.g., operating the flow electrolysis cell in recirculation mode, as the gas produced by the reaction can be continuously released from the solution reservoir. However, high conversion in a single pass, even for gas releasing reactions, is highly desirable,<sup>[8–10]</sup> especially considering that a large amount of anodic oxidations release  $\text{H}_2$  as byproduct from the cathode.

Under the conditions that provided the highest yield of **2** (200  $\mu\text{L}/\text{min}$ , 3 F/mol, 96 mA), the reactor was run for 150 min (30 mL volume). The conversion and yield were stable during the long run. No drop of the reaction conversion or selectivity due to e.g. electrode fouling could be detected. The high selectivity of the reaction allowed for a relatively simple workup of the crude reaction mixture. Thus, the solution collected from the reactor output was evaporated under reduced pressure and the remaining salts precipitated by adding dichloromethane. The solid was filtered off and the solvent was evaporated, yielding the pure product **2** (85%).

### 3. Conclusions

In summary, we have designed and developed a flow electrolysis cell based on a parallel plate arrangement. The setup can be easily assembled and consists of two flat  $5 \times 5$  cm electrodes separated by laser-cut Mylar plastic foils incorporating a flow channel and a series of additional Mylar films acting as gaskets and insulating material. The use of inexpensive laser cutting techniques avoids the need of CNC machining, and enables the incorporation of customized flow channels with mixing geometries. This versatile flow cell can accommodate electrodes of a wide range of thicknesses, and can be operated in divided and undivided mode.

The performance of the cell has been assessed using the anodic decarboxylative methoxylation of diphenylacetic acid (**1**) as model. Initial experiments have demonstrated that the incorporation of mixing geometries in the flow channel can improve the current efficiency of the reactor. Moreover, excellent yields were achieved in a single pass of the reaction mixture through the cell.

Several flow electrolysis cells with similar designs have been previously described in the literature.<sup>[10]</sup> The aim of this work is to provide an efficient design that is inexpensive, simple to assemble, and easy to reproduce. For this reason, extensive details are provided in the Supporting Information, including graphical guides, technical drawings, and the CAD and scalable vector files necessary for the construction of the cell.

## Experimental Section

### General Information

$^1\text{H}$  NMR spectra were recorded on a 300 MHz instrument.  $^{13}\text{C}$  NMR spectra were recorded on the same instrument at 75 MHz. Chemical shifts ( $\delta$ ) are expressed in ppm downfield from TMS as internal standard. The letters s, d, t, q, and m are used to indicate singlet, doublet, triplet, quadruplet, and multiplet, respectively. HPLC analysis was carried out on a C18 reversed-phase analytical column ( $150 \times 4.6$  mm, particle size 5  $\mu\text{m}$ ) at 37  $^\circ\text{C}$  using mobile phases: A (water/MeCN 90:10 (v/v) + 0.1% TFA) and B (MeCN + 0.1% TFA) at a flow rate of 1.5 mL/min. The following gradient was applied: 30 to 100% B from 0 to 10 min. All chemicals were obtained from standard commercial vendors and were used without any further purification.

### Electrochemical Decarboxylative Methoxylation of Diphenylacetic acid.

*General Procedure A: Batch.* 3 mL of a solution of **1** (0.1 M) and NaOMe (0.05 M) in methanol were introduced in a 5 mL IKA Electrasyn vial equipped with a graphite anode and a stainless steel cathode. The solution was electrolyzed under a constant current of 15 mA. After 2 F/mol of charge had been passed, the reaction mixture was monitored by HPLC (93% HPLC yield).

*General Procedure B: Flow Single-pass.* A solution of **1** (0.1 M) and NaOMe (0.05 M) in methanol was pumped through the continuous flow electrolysis cell using a peristaltic pump as depicted in Figure 3. The reactor was operated under constant current mode using a PeakTech 6225 A power supply. After the reactor had reached steady-state conditions, aliquots of the crude reaction mixture were collected from the reactor output and analyzed by HPLC.

*General Procedure C: Flow Recirculation.* A 0.1 M solution of **1** and NaOMe (0.05 M) in 40 mL of methanol was recirculated through the electrolysis cell at a flow rate of 2.5 mL/min. For this purpose, two peristaltic pumps were utilized (1.25 mL/min each). The reactor was operated under constant current mode (256 mA) using a PeakTech 6225 A power supply until the desired amount of charge was passed to the reagent solution. Then, the reactor inlet was removed from the electrolyte reservoir allowing air to enter the reactor and flush all the remaining reaction mixture to the vessel. Aliquots (50  $\mu\text{L}$ ) of the reaction mixture were collected from the reservoir during cell operation to monitor the reaction progress by HPLC.

**Synthesis of Benzhydrol methyl ether (2):** Following the single-pass flow electrolysis described above, a 0.1 M solution of **1** in MeOH and 0.05 M NaOMe was pumped through the continuous flow electrolysis cell at a flow rate of 200  $\mu\text{L}/\text{min}$ . The reactor was operated under constant current mode (96 mA). After reaching steady-state conditions, 30 mL (3 mmol scale) of the crude reaction mixture were collected from the reactor output. The solvent was evaporated under reduced pressure and the residue treated with dichloromethane. The solid was filtered off and the solution evaporated under reduced pressure, yielding 505 mg (85% isolated yield) of the spectroscopically pure title compound as a colorless oil.  $^1\text{H}$  NMR (300 MHz, Chloroform-*d*)  $\delta$  7.42–7.26 (m, 10H), 5.29 (s, 1H), 3.43 (s, 3H).  $^{13}\text{C}$  NMR (75 MHz, Chloroform-*d*)  $\delta$  142.2, 128.5, 127.6, 127.0, 85.6, 57.2. MS-EI:  $m/z$  198 (50%), 167 (62%), 121 (100%), 105 (60%), 77 (79%).

### Acknowledgements

The CCFLOW project (Austrian Research Promotion Agency FFG No. 862766) is funded through the Austrian COMET Program by the Austrian Federal Ministry of Transport, Innovation and Technology (BMVIT), the Austrian Federal Ministry of Digital and Economic Affairs (BMDW) and by the State of Styria (Styrian Funding Agency SFG).

### Conflict of Interest

The authors declare no conflict of interest.

**Keywords:** flow electrolysis cell • electroorganic synthesis • microreactors • anodic oxidation • methoxylation

- [1] *Organic Electrochemistry. Revised and Expanded, 5<sup>th</sup> Edn.* (O. Hammerich, B. Speiser, Eds.), CRC Press, Boca Raton, 2015.
- [2] a) A. Wiebe, T. Gieshoff, S. Möhle, E. Rodrigo, M. Zirbes, S. R. Waldvogel, *Angew. Chem. Int. Ed.* **2018**, *57*, 5594–5619; *Angew. Chem.* **2018**, *130*, 5694–5721; b) A. Shatskiy, H. Lundberg, M. D. Kärkäs, *ChemElectroChem* **2019**, *6*, 4067–4092.
- [3] a) H. J. Schäfer, *C. R. Chimie*, **2011**, *14*, 745–765; b) E. J. Horn, B. R. Rosen, P. S. Baran, *ACS Cent. Sci.* **2016**, *25*, 302–308.
- [4] a) M. Yan, Y. Kawamata, P. S. Baran, *Chem. Rev.* **2017**, *117*, 13230–13319; b) P. G. Echeverria, D. Delbrayelle, A. Letort, F. Nomertin, M. Perez, L. Petit, *Aldrichimica Acta*, **2018**, *51*, 3–19.
- [5] D. Pletcher, *Electrochem. Commun.* **2018**, *88*, 1–4.
- [6] a) M. Yan, Y. Kawamata, P. S. Baran, *Angew. Chem. Int. Ed.* **2018**, *57*, 4149–4155; *Angew. Chem.* **2018**, *130*, 4219–4225; b) C. Kingston, M. D. Palkowitz, Y. Takahira, J. C. Vantourout, B. K. Peters, Y. Kawamata, P. S. Baran, *Acc. Chem. Res.* **2020**, *53*, 72–83.
- [7] D. Pletcher, F. C. Walsh, *Industrial Electrochemistry, Second Edition*, Springer, Dordrecht, Netherlands, 1993.
- [8] D. Pletcher, R. A. Green, R. C. D. Brown, *Chem. Rev.* **2018**, *118*, 4573–4591.
- [9] a) M. Atobe, H. Tateno, Y. Matsumura, *Chem. Rev.* **2018**, *118*, 4541–4572; b) T. Noël, Y. Cao, G. Laudadio, *Acc. Chem. Res.* **2019**, *52*, 10, 2858–2869; c) K. Watts, A. Baker, T. Wirth, *J. Flow Chem.* **2014**, *4*, 2–11; d) Y.-i. Yoshida, *Electrochem. Soc. Interface* **2009**, *18*, 40–45; e) T. P. Nicholls, C. Schotten, C. E. Willans, *Curr. Opin. Green Sustain. Chem.* **2020**, *26*, 100355.
- [10] S. Maljuric, W. Jud, C. O. Kappe, D. Cantillo, *J. Flow Chem.* **2020**, *10*, 181–190.
- [11] a) A. A. Folguez-Amador, K. Philipps, S. Guilbaud, J. Poelakker, T. Wirth, *Angew. Chem. Int. Ed.* **2017**, *56*, 15446–15450; *Angew. Chem.* **2017**, *129*, 15648–15653; b) N. Amri, R. A. Skilton, D. Guthrie, T. Wirth, *Synlett* **2019**, *30*, 1183–1186; c) M. Kupper, V. Hessel, H. Lowe, W. Stark, J. Kinkel, M. Michel, H. Schmidt-Traub, *Electrochim. Acta* **2003**, *48*, 2889–2896; d) M. R. Chapman, Y. M. Shafi, N. Kapur, B. N. Nguyen, C. E. Willans, *Chem. Commun.* **2015**, *51*, 1282–1284; e) J. Kuleshova, J. T. Hill-Cousins, P. R. Birkin, R. C. D. Brown, D. Pletcher, T. J. Underwood, *Electrochim. Acta* **2012**, *69*, 197–202; f) J. Kuleshova, J. T. Hill-Cousins, P. R. Birkin, R. C. D. Brown, D. Pletcher, T. J. Underwood, *Electrochim. Acta* **2011**, *56*, 4322–4326; g) G. Laudadio, W. de Smet, L. Struik, Y. Cao, T. Noël, *J. Flow Chem.* **2018**, *8*, 157–165; h) Y. Mo, Z. Lu, G. Rughoobur, P. Patil, N. Gershenfeld, A. I. Akinwande, S. L. Buchwald, K. F. Jensen, *Science* **2020**, *368*, 1352–1357.
- [12] For an alternative design based in a concentric electrodes arrangement from our laboratory, see: W. Jud, C. O. Kappe, D. Cantillo, *ChemElectroChem* **2020**, *7*, 2777–2783.
- [13] C. Spiegel, *Designing and Building Fuel Cells*, McGraw-Hill Professional, New York, 2007.
- [14] a) M. Finkelstein, R. C. Petersen, *J. Org. Chem.* **1960**, *25*, 136–137; b) A. J. v. d. Hoek, W. T. Nauta, *Rec. Trav. Chim.* **1942**, *61*, 845–849; c) R. P. Linstead, B. R. Shephard, B. C. L. Weedon, *J. Chem. Soc.* **1952**, 3624–3627.
- [15] H. Hofer, M. Moest, *Liebigs Ann.* **1902**, *323*, 284–323.
- [16] H.-J. Schäfer, *Top. Curr. Chem.* **1990**, *152*, 91–151.
- [17] For recent examples, see: a) D. E. Collin, A. A. Folguez-Amador, D. Pletcher, M. E. Light, B. Linclau, R. C. D. Brown, *Chem. Eur. J.* **2020**, *26*, 374–378; b) M. Santi, J. Seitz, R. Cicala, T. Hardwick, N. Ahmed, T. Wirth, *Chem. Eur. J.* **2019**, *25*, 16230–16235.
- [18] A. A. Folguez-Amador, A. E. Teuten, D. Pletcher, R. C. D. Brown, *React. Chem. Eng.* **2020**, *5*, 712–718.
- [19] V. Hessel, H. Löwe, F. Schönfeld, *Chem. Eng. Sci.* **2005**, *60*, 2479–2501.
- [20] C.-Y. Wu, R.-T. Tsai, *Chem. Eng. J.* **2013**, *217*, 320–328.
- [21] C. P. Holvey, D. M. Roberge, M. Gottsponer, N. Kockmann, A. Macchia, *Chem. Eng. Process.* **2011**, *50*, 1069–1075.

---

Manuscript received: August 2, 2020

Version of record online: September 17, 2020